

Observation of thresholds and overlapping resonances below the $10^2P_{1/2}$ and $2P_{3/2}$ thresholds in the photodetachment of Cs^-

A. O. Lindahl,¹ J. Rohlén,^{1,*} H. Hultgren,^{1,2} D. J. Pegg,³ C. W. Walter,⁴ and D. Hanstorp^{1,†}

¹*Department of Physics, University of Gothenburg, SE-412 96 Gothenburg, Sweden*

²*Albert-Ludwigs-Universität, D-79104 Freiburg, Germany*

³*Department of Physics, University of Tennessee, Knoxville, Tennessee 37996, USA*

⁴*Department of Physics and Astronomy, Denison University, Granville, Ohio 43023, USA*

(Received 5 June 2013; published 11 November 2013)

A collinear beam apparatus has been used to study photodetachment of Cs^- . Partial cross sections were measured using state-selective detection based on a resonance ionization scheme. Several resonances were observed in the $\text{Cs}(10^2S)$, $\text{Cs}(6^2F)$, $\text{Cs}(6^2G)$, and $\text{Cs}(6^2H)$ final-state channels below the $\text{Cs}(10^2P_{3/2})$ channel opening. A model was developed to account for the interference between overlapping resonances. This model is essentially a generalization of the Fano [U. Fano, *Phys. Rev.* **124**, 1866 (1961)] and Shore [B. W. Shore, *Phys. Rev.* **171**, 43 (1968)] parametrizations for single resonances. Resonance parameters were extracted by fitting the model to the data sets. The openings of the $\text{Cs}(10^2S)$ and $\text{Cs}(6^2F)$ channels, where the polarizabilities of the atomic states are large and positive, showed rapid onsets. In the case of the $\text{Cs}(6^2G)$ and $\text{Cs}(6^2H)$ channels, on the other hand, the photodetachment cross sections increased slowly with energy. For the $\text{Cs}(6^2H)$ channel this is the expected behavior, since it is the result of a large and negative polarizability of the 6^2H state. In addition, the excitation of the $\text{Cs}(6^2H)$ state with respect to the Cs ground state was found to be $28\,356.3(2)\text{ cm}^{-1}$, in agreement with a previous experiment.

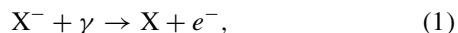
DOI: [10.1103/PhysRevA.88.053410](https://doi.org/10.1103/PhysRevA.88.053410)

PACS number(s): 32.80.Gc, 32.80.Zb, 32.80.Rm

I. INTRODUCTION

Negative ions are of considerable interest in the field of atomic physics. Their properties differ significantly from both positive ions and neutral systems. Electron-electron correlations are relatively more important in negative ions than in other systems due to the efficient screening of the nuclear charge. Studies of negative ions can therefore serve as benchmarks for many-body effects in atomic theory.

The asymptotic interaction in negative ions can be described by an induced dipole potential. It scales with distance as $1/r^4$, much shorter ranged than the $1/r$ -dependence of the Coulomb potential. In contrast to the infinite series of Rydberg states in a Coulomb potential, the induced dipole potential can typically support only a single state [1]. Spectroscopic properties of negative ions are often determined using photodetachment [5] which, for a general negative ion X^- , can be written as



where γ represents a photon and e^- an electron.

As stated above, bound electronically excited states typically do not exist in negative ions. However, above the first detachment limit there are rich spectra of doubly excited states [6]. Such states are bound with respect to excited states in the parent atom and are embedded in one or more single detachment continua. Electron-electron correlations have an even greater influence on the properties of these states than they have on the bound states of the ion. Doubly excited states in H^- , the most fundamental system, have been extensively investigated both theoretically and experimentally [7–11].

While H^- is a pure two-electron system, negative ions of the alkali metals can be considered to be effective two-electron systems in the sense that two active electrons move in the field of a closed, frozen core.

Previous experimental investigations of doubly excited states of alkali-metal negative ions include studies on Li^- [12,13], Na^- [14], K^- [15,16], Rb^- [17,18], and Cs^- [17,19].

The photodetachment cross section in the threshold region is commonly described by the so-called Wigner law [20]:

$$\sigma \propto E^{\ell+1/2}. \quad (2)$$

Here E and ℓ represent the energy and orbital angular momentum of the detached electron, respectively. Deviations from the Wigner law can be caused by either a nonzero polarizability of the residual atom [21] or the finite-size wave function of the initial system [22]. For photodetachment into ground-state atoms, with polarizabilities on the order of 10 a.u. , the description is typically valid up to several meV above the threshold [23,24].

It has been shown experimentally that larger positive polarizabilities reduce the range of validity of the Wigner law [25]. In addition, it was recently demonstrated that two thresholds with similar angular momenta (>1) and equally large polarizabilities (10^5 – 10^6 a.u.), but with opposite signs, show diametrically different behaviors. Comparing the two cross sections, the positive polarizability causes a sharp, steplike onset where a plateau in the cross section is reached within 0.5 meV , while the negative polarizability shows a slow and gradual onset over 50 meV [26].

Cs^- is the heaviest alkali-metal negative ion that can be studied without using a radioactive ion beam facility. It is a very complicated atomic system which poses a difficult challenge for current theories. Thus, it is of high interest

*johan.rohlen@physics.gu.se

†dag.hanstorp@physics.gu.se

to further examine the properties of Cs^- photodetachment in order to increase the understanding of many-electron systems.

So far, Cs^- photodetachment has been investigated up to 1.96 eV [19]. The upper limit of this photon energy range allows for an investigation of the photodetachment of Cs^- via a final-state channel that leaves the residual Cs atom in the first-excited state. A Feshbach resonance situated just below the $\text{Cs}(6^2P_{1/2})$ state suppresses the nonresonant photodetachment cross section by 2 orders of magnitude [19,27]. This fact was utilized in an excess-photon detachment study by Stapelfeldt and Haugen [28].

For a long time it was thought that the Cs^- ion might have a bound state with opposite parity to the ground state. Scheer *et al.* [29] proved this not to be the case when they observed the $\text{Cs}^-(6s6p\ ^3P)$ state, situated above the single detachment threshold. Prior to this observation, extensive theoretical work had been done on predicting the energy of the 3P states [27,30].

There exist few theoretical works on Cs^- photodetachment. However, Bahrim *et al.* [31] calculated the absolute photodetachment cross section within 80 meV of the ground-state threshold using the Pauli equation method. They were able to reproduce the 3P state as well as extracting other physical parameters such as asymmetry parameters.

The 10^2S and 6^2F states of Cs have polarizabilities of 4.75×10^5 and 7.77×10^6 a.u. [32], respectively. The polarizability of the 6^2F state is thus of the same order of magnitude as the 5^2F state in K, which was investigated in [26].

In the present paper the aim has been to extend the photodetachment energy range to higher-lying final states. Measurements of partial cross sections for photodetachment from Cs^- into the channels involving the 10^2S , 6^2F , 6^2G , and 6^2H final states of the residual atom are reported. A resonance parametrization method that takes account of overlapping resonances has been developed which enables extraction of resonance parameters from the measured cross-section data. In addition, the effect of the final-state polarizability on the shape of the threshold was investigated. The experiment was performed at GUNILLA (Göteborg University Negative Ion Laser Laboratory), where a resonance ionization scheme was utilized in order to measure the partial cross sections.

II. EXPERIMENT

A. Procedure

Figure 1 shows the optical excitation scheme used in the experiment. Cs^- ions were photodetached by uv photons with energies ranging from 3.976 to 4.038 eV. This is substantially larger than the electron affinity of Cs (0.471 626(25) eV [5]) and close to the energy needed for double detachment (4.365 531(25) eV [5,33]). All final states in the residual atom that are energetically available are populated in the process. State selectivity was achieved using a two-step resonant ionization scheme. First, the state of interest was resonantly excited by an ir photon to a highly excited Rydberg state which subsequently was ionized by an electric field. By detecting and counting the positive ions thus created, it was possible to measure specific partial cross sections. In the present experiment the following photodetachment channels

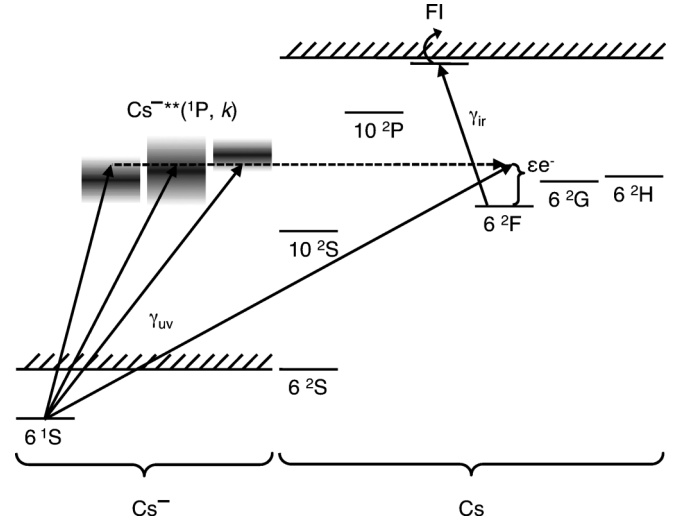
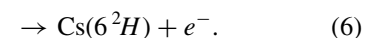
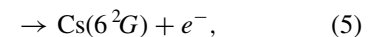
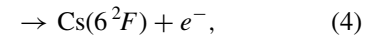
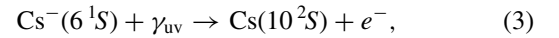


FIG. 1. Partial energy level diagram (not to scale) of the Cs^- and Cs systems. $\text{Cs}^-^{**}(^1P, k)$ represents the k th doubly excited state of the negative ion with 1P symmetry. In this example, a uv photon (γ_{uv}) detaches one electron from the Cs^- ion and excites the valence electron in the residual atom to the 6^2F state. Alternatively the ion is promoted to a doubly excited state, which decays via autodetachment (horizontal dashed arrow). The vertical curly bracket represents the kinetic energy of the detached electron. Although only transitions to the 6^2F state are shown, all energetically available states are populated. State selectivity in the detection is achieved by resonant excitation using an ir photon (γ_{ir}) followed by field ionization (FI).

were investigated:



These channels have threshold energies of 3.980 407(25), 3.984 025(25), 3.986 881(25), and 3.987 375(26) eV, respectively [5,33,34]. The uncertainties are comprised of the statistical uncertainties of the electron affinity and the relevant energy levels in Cs. The quoted uncertainty on the measured electron affinity of $25 \mu\text{eV}$ dominates [5]. It should be noted that Cs has a ground-state hyperfine splitting of $38 \mu\text{eV}$. Since the most accurate experiment on the electron affinity of Cs never was published [5], it is not known if the quoted value is referenced to the $F = 3$ true ground state of Cs or the weighted mean of the $F = 3$ and $F = 4$ states. This introduces an extra uncertainty of $21 \mu\text{eV}$ in the channel threshold positions. The threshold positions are only used as indicators of the channel openings in Figs. 3, 4, and 5. In the cases of the 6^2F and 6^2G states, the fine-structure splittings are 13 and $0.2 \mu\text{eV}$ [33], respectively, which are below the resolution of the experiment. The fine structure splitting of 6^2H is not known. The photon energy range used in the experiment encompasses the openings of the aforementioned channels, as well as the opening of the $\text{Cs}(10^2P_{1/2})$ channel at 4.033 296(25) eV and the $\text{Cs}(10^2P_{3/2})$ channel at 4.036 627(25) eV [5,33].

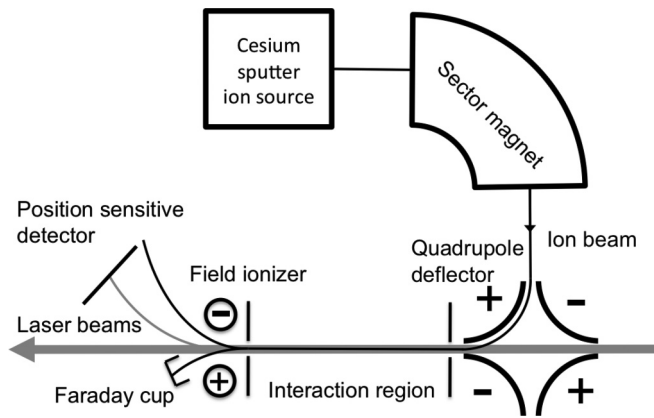


FIG. 2. A schematic of the collinear beams apparatus. Two laser beams and an ion beam are superimposed in a collinear copropagating geometry. Positive ions that enter the field ionizer are deflected away from the detector while ions produced by field ionization strike the detector.

B. Apparatus

Photodetachment of Cs^- was studied using the collinear beam apparatus at GUNILLA [35]. A large interaction volume defined by the overlap of collinearly superimposed ion and laser beams provided a highly sensitive measurement system. This was crucial since the partial photodetachment cross sections to highly excited states are generally very small as shown, for example, in [36]. Moreover, the energy separations of the states investigated in the Cs atom are on the order of meV, which necessitates high energy-resolution in the final-state detection. The state-selective detection of these atoms via resonance ionization was the basis for high selectivity. The energy resolution in the experiment was enhanced by the large reduction in kinematic broadening brought about by the collinear interaction of the ion and laser beams [37]. In the present measurement, the energy resolution was determined primarily by the finite bandwidth of the laser used for photodetachment, which was approximately $25 \mu\text{eV}$.

A schematic overview of the ion beam apparatus is shown in Fig. 2. The experimental arrangement has been described in detail in a recent publication [16]. Negative ions of cesium were produced in a cesium sputter ion source using a solid aluminium target. The Cs^- ions were accelerated to 6 keV energy. The ion beam was mass selected in a magnetic sector before it was guided by an electrostatic quadrupole deflector into an interaction region defined by two 3-mm apertures placed 61 cm apart. The ion optical design of the apparatus has been described in detail by Diehl *et al.* [35]. The interaction region is shielded against stray electric fields by means of a stainless steel tube centered along the path of the ions. In the interaction region the ion beam was merged with two copropagating laser beams. One was used for photodetachment and the other for resonant excitation in the detection process.

After the interaction region, an inhomogeneous electric field and a position-sensitive detector served as a Rydberg-state analyzer. The highly excited Rydberg atoms, created by resonant excitation, were field ionized and the resulting

positive ions were deflected by the same field. The positive ions were detected by the position-sensitive detector. The inhomogeneous field in the field ionizer helped to separate the signal from the major source of background, namely, positive ions created in the interaction region by sequential photodetachment-photoionization by two uv photons [16].

The uv and ir radiation were generated by two laser systems, each utilizing a series of nonlinear optical processes such as doubling, tripling, and optical parametric oscillators. Both laser systems were pumped by Nd:YAG lasers which operated at a repetition rate of 10 Hz. The spectral bandwidth was $25 \mu\text{eV}$ and the pulse length was a few nanoseconds.

Each laser system has several outputs that deliver light of different wavelengths. It was sufficient to measure the wavelength of the pump laser and one visible output of a laser system in order to determine the wavelength of any other output.

The pulse energy of the ir laser after the chamber was approximately 0.2 mJ, which was sufficient to saturate the resonant transitions to the Rydberg states. The uv pulse energy was approximately 0.7 mJ, far from saturating the nonresonant photodetachment process.

In order to investigate the cross sections, the uv radiation was tuned from 3.976 to 4.038 eV in the ion rest frame. For the various channels studied, the ir laser was tuned to the resonant transitions $10^2S \rightarrow 24^2P$, $6^2F \rightarrow 24^2D$, $6^2G \rightarrow 23^2F$ or $6^2H \rightarrow 20^2G$, which, in the rest frame, lie between 344 and 353 meV [33,34]. The uv pulse arrived at the interaction region approximately 20 ns before the ir pulse.

The negative ion beam was deflected into a Faraday cup by the field ionizer. The ion beam current, after the passage through the interaction region, was on the order of 1 nA. For each shot of the two lasers, the data from the position-sensitive detector were recorded together with the measured wavelength, the pulse energy of the uv radiation, and the ion current.

The data analysis was performed using an off-line procedure. Data was binned according to the measured photon energy of the uv radiation. Each bin corresponds to a data point in a cross-section curve. An estimate of the diffuse background on the detector that was observed in the experiment was performed by calculating the mean hit density around the signal peak. The number of hits in the signal peak was then integrated and the background was subtracted. The number of hits was normalized with respect to the ion current, the pulse energy of the uv laser, and the number of laser shots in the bin.

Unfortunately, variations in the overlap between the two laser beams and the ion beam necessitated a separate normalization of the different data sets to be able to sum them. Thus, the vertical scales in Figs. 3, 4, and 5 are not comparable. However, based on the normalized count rates, the cross sections in the different channels are of the same order of magnitude.

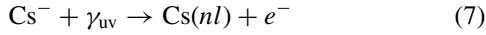
The measured laboratory-frame photon energies were converted to energies in the ion rest frame by use of the known kinetic energy of the ion beam. This Doppler shift correction introduced an uncertainty in the photon energy of the uv radiation of less than $10 \mu\text{eV}$, which is less than half of the laser bandwidth.

C. Analysis of overlapping resonances

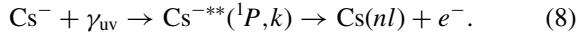
The presence of doubly excited states in the single detachment continuum in a negative ion gives rise to resonances in the photodetachment cross section. Fano [38] derived an analytical expression that describes the modulation of a cross section in the presence of a single resonance. Later, Shore [39] deduced an equivalent expression, which is an alternative parametrization of the shape described by the Fano profile.

In the present study, a number of overlapping resonances are observed. Due to the interaction of the resonances, neither Fano nor Shore profiles can be used to correctly describe the observed cross sections. In order to extract energies and widths for the observed resonances a numerical method is used which takes the interference of the resonances into account. The interaction between resonances via a continuum can in principle modify the energies and widths of the resonant states. Such effects are not taken into account in the present model and thus only the modified parameters can be accessed.

The transition amplitude from the initial to the final state has contributions from the direct path



and the resonant paths (shown in Fig. 1)



Here $\text{Cs}^{-**}(^1P, k)$ represents $k = 1, 2, 3, \dots, N$ doubly excited states of 1P symmetry and $\text{Cs}(nl)$ a specific final state.

We let the transition amplitude for the direct process in Eq. (7) be represented by a real amplitude, $A_{nl}(\hbar\omega)$, where $\hbar\omega$

is the photon energy of the uv laser. The complex transition amplitude for each resonant path in Eq. (8) is represented by a real amplitude, $\tilde{C}_{nl}^k(\hbar\omega)$, and a pole in the complex plane:

$$B_{nl}^k(\hbar\omega) = \frac{\tilde{C}_{nl}^k(\hbar\omega)}{\hbar\omega - E_k + i\frac{\Gamma_k}{2}}, \quad (9)$$

where E_k and Γ_k are the energy and width of the k th resonance. By introducing the dimensionless energy parameter $\epsilon_k = (\hbar\omega - E_k)/\frac{\Gamma_k}{2}$ and $C_{nl}^k(\hbar\omega) = \tilde{C}_{nl}^k(\hbar\omega)/\frac{\Gamma_k}{2}$, the complex amplitude $B_{nl}^k(\hbar\omega)$ can be expressed as

$$B_{nl}^k(\hbar\omega) = \frac{C_{nl}^k(\hbar\omega)}{\epsilon_k + i}. \quad (10)$$

The total amplitude for the photodetachment reaction, T_{nl} , can then be expressed as

$$T_{nl}(\hbar\omega) = \left(A_{nl}(\hbar\omega) + \sum_{k=1}^N \frac{C_{nl}^k(\hbar\omega)e^{i\delta_{nl}^k}}{\epsilon_k + i} \right) \quad (11)$$

if the intrinsic phase shift between the direct and the resonant paths, δ_{nl}^k , is included. The phase shift for each resonance is assumed to be constant and it is determined in the fit. The energy dependence of $C_{nl}^k(\hbar\omega)$ comes from the variation of the fractional branching of the $\text{Cs}^{-**}(^1P, k)$ state population into the $\text{Cs}(nl)$ state, i.e., the probability for the second step of Eq. (8). To proceed further, and in order to arrive at a familiar result, we assume that the energy dependence of the branching is the same as the energy dependence of the nonresonant cross section. With this assumption, the ratio $C_{nl}^k(\hbar\omega)/A_{nl}(\hbar\omega) = s_{nl}^k$

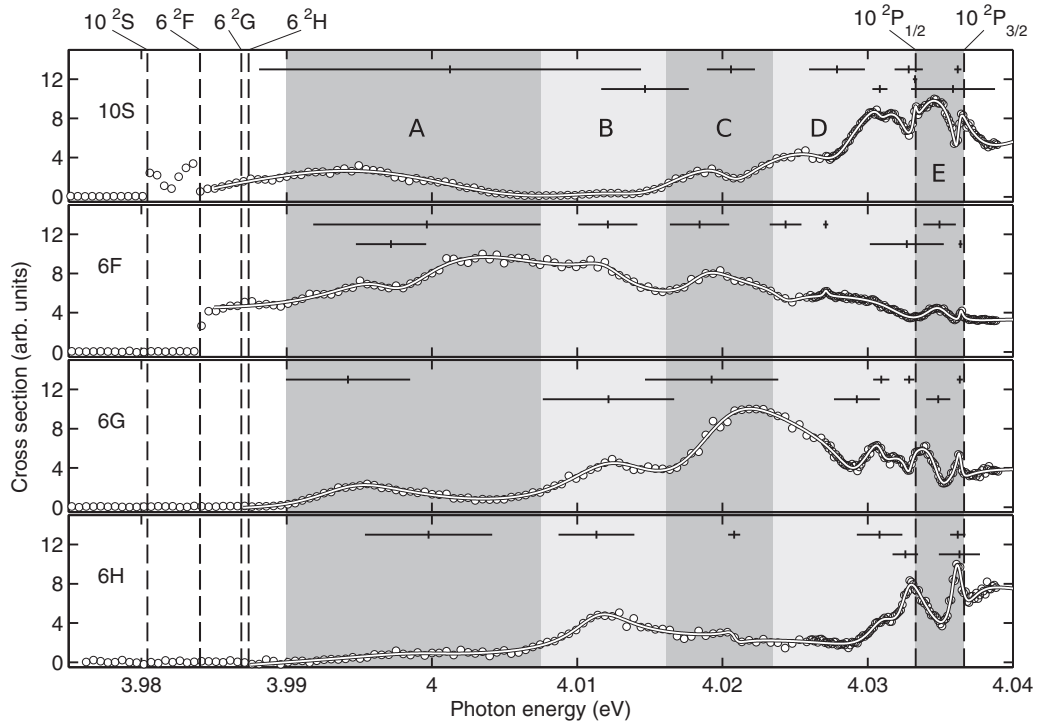


FIG. 3. Partial cross section in the 10^2S , 6^2F , 6^2G , and 6^2H channels. Dashed vertical lines mark threshold energies with state assignments shown at the top of the figure. Resonance parameters extracted from the fits are shown in the respective panels. Resonance energies are shown as short vertical lines, while the horizontal lines represent widths. Regions A, B, C, D, and E are used as guides for the discussion of the observed resonances in Sec. IV. The cross sections obtained by fitting Eq. (12) to the data are shown as solid curves. For a detailed view of regions D and E, see Fig. 4.

is constant and represents the relative amplitude of the resonant path compared to the direct path.

The reaction cross section is given by $\sigma_{nl} = |T_{nl}|^2$. By introducing s_{nl}^k , this can be expressed as

$$\sigma_{nl} = A_{nl}^2 \left| 1 + \sum_{k=1}^N \frac{s_{nl}^k e^{i\delta_{nl}^k}}{\epsilon_k + i} \right|^2. \quad (12)$$

This expression can easily be implemented numerically in a standard fitting routine. In such a fit, an analytical form of the nonresonant cross section has to be selected. The parameters determined in the fit are the energy E_k , the width Γ_k , the phase shift δ_{nl}^k , the relative amplitude s_{nl}^k for each resonance, and the free parameters connected to the nonresonant cross section.

A description of overlapping resonances should, of course, reproduce the established expressions for a single isolated resonance. Therefore, the sum in Eq. (12) is evaluated with $N = 1$. For a single resonance, the calculation of the cross section can be performed analytically and results in

$$\sigma_{nl} = A_{nl}^2 \left(1 + \frac{\epsilon 2 s_{nl} \cos(\delta_{nl}) + (s_{nl})^2 + 2 s_{nl} \sin(\delta_{nl})}{\epsilon^2 + 1} \right), \quad (13)$$

where the index $k = 1$ has been dropped.

By substituting $a = 2 s_{nl} \cos(\delta_{nl})$ and $b = (s_{nl})^2 + 2 s_{nl} \sin(\delta_{nl})$ into Eq. (13) the well-known expression

$$\sigma_{nl} = A_{nl}^2 \left(1 + \frac{\epsilon a + b}{\epsilon^2 + 1} \right) \quad (14)$$

is obtained, which, for example, was used in [40]. The expression in Eq. (13) thus represents an alternative parametrization with the same result as the Shore [39] and Fano [38] profiles in the limit of a single resonance.

III. RESULTS

Partial photodetachment cross sections for the Cs(10^2S), Cs(6^2F), Cs(6^2G), and Cs(6^2H) channels are shown in Fig. 3. Data are presented with two different resolutions. Up to 4.027 eV, the data have a bin size of 4 cm^{-1} ($\approx 496 \mu\text{eV}$), while above 4.027 eV, the data have a bin size of 1 cm^{-1} ($\approx 124 \mu\text{eV}$).

Two regions in Fig. 3 contain features of interest that are shown in more detail in separate figures. Figure 4 contains the region encompassing the Cs($10^2P_{1/2,3/2}$) channel openings. It has a bin size of 1 cm^{-1} ($\approx 124 \mu\text{eV}$). Figure 5 shows the cross section of the Cs(10^2S) channel from threshold to above the Cs(6^2F) channel opening with a bin size of 0.2 cm^{-1} ($\approx 25 \mu\text{eV}$).

The cross section in Fig. 5 has a very sharp onset, plateauing after only 0.16 meV. In this energy range, the Wigner law can be fitted to the observed cross section. It is then strongly modulated before it is reduced by 85% over a range of 0.5 meV, just below the opening of the Cs(6^2F) channel. The cross section then increases slowly up to an energy of 3.994 eV. Right at the opening of the Cs(6^2F) channel, a very narrow structure is observed.

The cross section for the Cs(6^2F) channel also has a sharp onset, plateauing after 1.1 meV. Due to the limited resolution, no threshold law can be fitted to the data.

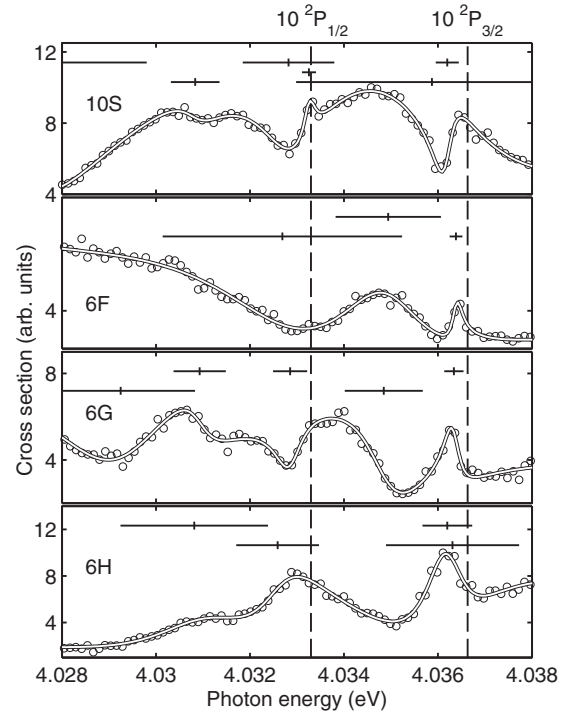


FIG. 4. Detailed view of the region of the Cs($10^2P_{1/2,3/2}$) channel openings from Fig. 3. Dashed vertical lines mark threshold energies with state assignments shown at the top of the figure. Resonance parameters extracted from the fits discussed in Sec. IV are shown in the respective panels. Resonance energies are shown as short vertical lines, while the horizontal lines represent widths. The cross sections obtained by fitting Eq. (12) to the data are shown as solid curves.

For the Cs(6^2G) and Cs(6^2H) channels, on the other hand, the cross section rises much more slowly above threshold, plateauing after approximately 10 meV for both channels. For these two channels the noise in the data makes it impossible to determine if the Wigner law or the threshold law developed in [20] gives the better fit.

All four partial cross sections show large modulations, indicating the presence of a number of resonances which are discussed in Sec. IV.

This experiment constitutes only the second independent observation of the 6^2H state in Cs [34,41]. Thus, it is of interest to discuss the details of the second step in the detection

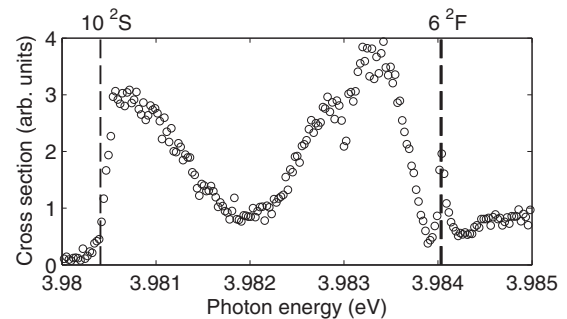


FIG. 5. Partial cross section in the Cs(10^2S) channel in the threshold region. Dashed vertical lines mark the threshold energies. Bin size is 0.2 cm^{-1} .

scheme for the Cs(6^2H) channel. In this step, ir photons are used to excite Cs atoms from the 6^2H state into the 20^2G state. By measuring this transition energy and subtracting it from the known energy of the 20^2G state, the energy of the 6^2H state can be determined. The uv photon energy was kept fixed at a value that ensured photodetachment into the 6^2H channel. The transition energy to the 20^2G state was then measured by manually adjusting the ir photon energy to maximize the resonant population transfer to the 20^2G state. Due to the procedure, the uncertainty in the determination was almost equal to the bandwidth of the laser, which is 0.2 cm^{-1} . This energy was converted to the rest frame of the ions using the calculated Doppler shift. Note that the Doppler shift uncertainty is about ten times smaller in the ir compared to the uv due to the difference in photon energy.

The transition between the 6^2H and 20^2G states was determined to have an energy of $2\,775.6(2) \text{ cm}^{-1}$ in the rest frame of the atom. The energy of the 6^2H states is given by subtracting the transition energy from the known energy of the 20^2G state at $31\,131.935\,70(15) \text{ cm}^{-1}$ [33]. The result is $28\,356.3(2) \text{ cm}^{-1}$, which is in good agreement with the value by Civiš *et al.* of $28\,356.426(45) \text{ cm}^{-1}$ [41].

IV. DISCUSSION

The cross sections just above the thresholds in the Cs(10^2S) and Cs(6^2F) channels are steeply rising. This is in good agreement with previously measured photodetachment channels in which the residual atomic states have large positive polarizabilities [25,26]. The calculated polarizabilities of the 10^2S and 6^2F states are indeed very high, 4.75×10^5 and 7.77×10^6 a.u., respectively [32]. The polarizabilities of the 6^2G and 6^2H states are unknown. However, since the 6^2H state is the last in the series with principal quantum number $n = 6$ and it lies above the 6^2G state, the 6^2H state is expected to have a large and negative polarizability. The situation for the polarizability of the 6^2G state is more complicated since it interacts with both the 6^2F and 6^2H states with negative and positive contributions, respectively. Since the dipole overlaps of the different wave functions are unknown, it is difficult to predict even the sign of the polarizability without a complete calculation. The onset of the Cs(6^2H) channel shows a very slow onset of the cross section. This is in qualitative agreement with the observed behavior in K^- photodetachment into the K(5^2G) channel [26], where the negative polarizability determined the shape. Similarly, the cross section of the Cs(6^2G) channel also shows a slow onset. In this case it cannot be determined if the suppression is caused by a large negative polarizability or by the large angular momentum of the 6^2G state which, according to the Wigner law [Eq. (2)], gives rise to a slow onset.

The cross section in the Cs(10^2S) channel shows very large modulations in the 4 meV region between its threshold and the opening of the Cs(6^2F) channel (see Fig. 5). We have not been able to model the observed cross section. A single Shore profile could, however, be fitted to the sharp structure at the Cs(6^2F) channel opening. This resulted in an energy of $3.984\,040(11) \text{ eV}$ and a width of $95(11) \mu\text{eV}$. The main contribution to the uncertainty in the position arises from the uncertainty in the Doppler shift correction. It has not been possible to

determine if the measured energy of the resonance is below or above the threshold of the Cs(6^2F) channel, which is given as $3.984\,025(25) \text{ eV}$ in the literature [5,33]. Nonetheless, the most likely origin of this structure is a doubly excited state of Cs^- that is bound with respect to the parent Cs(6^2F) state.

The data shown in Fig. 3 clearly contain a number of resonances. Many of the resonances are too close to each other to be treated as isolated. Therefore, the numerical model described in Sec. II C was fitted to the data. Linear functions were used to describe the nonresonant cross sections in all cases. At least nine different resonance structures can be seen in the regions. As expected, some of these resonances are not visible in all four channels due to different branching from the doubly excited states to the final states in the atom. Attempts to fit expressions with the same number of resonances in all channels resulted in unstable fits. Instead, the minimum number of resonances needed to reproduce the experimental data was used in each channel. Resonance energies and widths extracted for each partial cross section are shown in the corresponding sections of Figs. 3 and 4.

Resonances in the cross sections are due to doubly excited states in the negative ion. These states have definite energies and widths, parameters that cannot be influenced by the different detachment channels. Extracting these parameters from different measured partial cross sections should thus yield the same values. In Figs. 3 and 4 this is not the case, and this fact gives an indication of the uncertainties in the identification of the resonances. To illustrate this we give the extracted parameters for resonances lying above 4.032 eV in all channels in Table I.

Figure 3 shows that there must be at least two resonances in region A. Although one resonance is enough to describe three of the partial cross sections in this region, the modulations in the Cs(6^2F) channel require two resonances. For the resonance in region B there is fairly good agreement in all the channels, concerning both the energy and the width. It is only in the Cs(10^2S) channel that the energy of the resonance is a bit larger than in the other channels. In region C there is reasonable agreement between the first three channels for the parameters

TABLE I. Resonance parameters for observed resonances lying above 4.032 eV . 1σ confidence bounds from the fitting routine are given in parentheses.

Channel	E_k (eV)	Γ_k (meV)
Cs(10^2S)	4.032 8(3)	1.9(5)
	4.033 25(4)	0.30(11)
	4.035 9(6)	5.8(9)
	4.036 196(24)	0.49(5)
Cs(6^2F)	4.032 7(7)	5.1(13)
	4.034 9(3)	2.2(7)
	4.036 38(5)	0.27(14)
Cs(6^2G)	4.032 85(8)	0.72(15)
	4.034 85(11)	1.7(2)
	4.036 34(4)	0.41(7)
Cs(6^2H)	4.032 59(15)	1.8(3)
	4.036 20(10)	1.1(2)
	4.036 3(5)	2.8(8)

of a single resonance. In the Cs(6^2H) channel on the other hand, the observed structure is much narrower than that in the other channels. It is thus likely that there are actually two resonances present in this region: one narrow, which is visible in the Cs(6^2H) channel, and one wider, which is more pronounced in the other channels. In region D there is seemingly much disagreement between the channels. However, between 4.03 eV and the Cs($10^2P_{1/2}$) opening, two of the resonances align well in the Cs(10^2S), Cs(6^2G), and Cs(6^2H) channels. Just below the Cs($10^2P_{3/2}$) channel opening in region E there is one resonance that is present at the same energy in all four channels, although the widths vary slightly. A second resonance is also present in all channels in this region, but for this one the variation in energy is rather large.

V. CONCLUSIONS

We have performed a high-resolution measurement of four partial cross sections for the photodetachment of the Cs⁻ ion into final-state channels that involve highly excited states of the residual Cs atom. In the cases where the final states have large positive polarizabilities (10^2S and 6^2F), the cross sections exhibit sharp thresholds at the channel openings. This is in agreement with what has been previously observed in the photodetachment of other negative ions of the alkali metals under similar conditions [25,26]. The 6^2H state is expected to have a negative polarizability and the corresponding channel shows a slow onset of the cross section. This is the same general behavior as previously observed at the opening of the K(5^2G) channel in K⁻ photodetachment [26]. For the 6^2G state in Cs, the value of the polarizability is unknown, but the cross section

is in agreement with either a small polarizability of any sign or a large and negative polarizability. Clearly, calculations of the polarizabilities of the 6^2G and 6^2H states would be of great interest for understanding the threshold behavior.

The cross sections in the four measured channels are modulated by the presence of many resonances below the Cs($10^2P_{1/2,3/2}$) channel openings. A tentative identification and assignment of the parameters of these resonances was made using a model that takes interference between resonances into account. Unfortunately, the parametrization of resonance profiles used in the analysis of the data does not allow an unambiguous identification of all the doubly excited states that are responsible for the modulations seen in the cross sections. Nevertheless, several resonances align well and useful resonance parameters can be extracted. The Cs⁻ ion is a heavy, many-electron system where electron correlation and relativistic effects play a crucial role in the structure and dynamics of the system. Clearly, a definite identification of the resonances observed in the current experiment would require *ab initio* calculations that take these effects into account. Such calculations would pose a formidable challenge and, at present, no such calculations have been performed.

ACKNOWLEDGMENTS

Financial support from the Swedish Research Council is gratefully acknowledged. C.W.W. received support from the Wenner-Gren Foundation, the Andrew W. Mellon Foundation, and NSF Grants No. 0757976 and No. 1068308. H.H. acknowledges the support by the Deutsche Forschungsgemeinschaft, Grant No. KI 865/3-1.

-
- [1] The only known exceptions which do have electronically excited states of opposite parity are Os⁻ [2] and Ce⁻ [3,4].
 - [2] R. C. Bilodeau and H. K. Haugen, *Phys. Rev. Lett.* **85**, 534 (2000).
 - [3] C. W. Walter, N. D. Gibson, C. M. Janczak, K. A. Starr, A. P. Snedden, R. L. Field, and P. Andersson, *Phys. Rev. A* **76**, 052702 (2007).
 - [4] C. W. Walter, N. D. Gibson, Y. G. Li, D. J. Matyas, R. M. Alton, S. E. Lou, R. L. Field, D. Hanstorp, L. Pan, and D. R. Beck, *Phys. Rev. A* **84**, 032514 (2011).
 - [5] T. Andersen, H. K. Haugen, and H. Hotop, *J. Phys. Chem. Ref. Data* **28**, 1511 (1999).
 - [6] D. J. Pegg, *Radiat. Phys. Chem.* **70**, 371 (2004).
 - [7] S. I. Themelis, *J. Chem. Phys.* **132**, 154111 (2010).
 - [8] E. Lindroth and J. L. Sanz-Vicario, *Radiat. Phys. Chem.* **70**, 387 (2004).
 - [9] P. Balling, H. H. Andersen, C. A. Brodie, U. V. Pedersen, V. V. Petrunin, M. K. Raarup, P. Steiner, and T. Andersen, *Phys. Rev. A* **61**, 022702 (2000).
 - [10] H. R. Sadeghpour and C. H. Greene, *Phys. Rev. Lett.* **65**, 313 (1990).
 - [11] P. G. Harris, H. C. Bryant, A. H. Mohagheghi, R. A. Reeder, H. Sharifian, C. Y. Tang, H. Tootoonchi, J. B. Donahue, C. R. Quick, D. C. Risllove, W. W. Smith, and J. E. Stewart, *Phys. Rev. Lett.* **65**, 309 (1990).
 - [12] U. Ljungblad, D. Hanstorp, U. Berzinsh, and D. J. Pegg, *Phys. Rev. Lett.* **77**, 3751 (1996).
 - [13] G. Haeffler, I. Y. Kiyani, U. Berzinsh, D. Hanstorp, N. Brandefelt, E. Lindroth, and D. J. Pegg, *Phys. Rev. A* **63**, 053409 (2001).
 - [14] G. Haeffler, I. Y. Kiyani, D. Hanstorp, B. J. Davies, and D. J. Pegg, *Phys. Rev. A* **59**, 3655 (1999).
 - [15] I. Y. Kiyani, U. Berzinsh, J. Sandström, D. Hanstorp, and D. J. Pegg, *Phys. Rev. Lett.* **84**, 5979 (2000).
 - [16] A. O. Lindahl, J. Rohlén, H. Hultgren, I. Y. Kiyani, D. J. Pegg, C. W. Walter, and D. Hanstorp, *Phys. Rev. A* **85**, 033415 (2012).
 - [17] T. A. Patterson, H. Hotop, A. Kasdan, D. W. Norcross, and W. C. Lineberger, *Phys. Rev. Lett.* **32**, 189 (1974).
 - [18] P. Frey, F. Breyer, and H. Hotop, *J. Phys. B: At. Mol. Phys.* **11**, L589 (1978).
 - [19] J. Slater, F. H. Read, S. E. Novick, and W. C. Lineberger, *Phys. Rev. A* **17**, 201 (1978).
 - [20] E. P. Wigner, *Phys. Rev.* **73**, 1002 (1948).
 - [21] T. F. O'Malley, *Phys. Rev.* **137**, A1668 (1965). Note the error in the sign of the correction factor, see, for example, Ref. [24].
 - [22] J. W. Farley, *Phys. Rev. A* **40**, 6286 (1989).
 - [23] R. C. Bilodeau, M. Scheer, H. K. Haugen, and R. L. Brooks, *Phys. Rev. A* **61**, 012505 (1999).
 - [24] H. Hotop, T. A. Patterson, and W. C. Lineberger, *Phys. Rev. A* **8**, 762 (1973).

- [25] J. Sandström, G. Haeffler, I. Y. Kiyan, U. Berzinsh, D. Hanstorp, D. J. Pegg, J. C. Hunnell, and S. J. Ward, *Phys. Rev. A* **70**, 052707 (2004).
- [26] A. O. Lindahl, J. Rohlén, H. Hultgren, I. Y. Kiyan, D. J. Pegg, C. W. Walter, and D. Hanstorp, *Phys. Rev. Lett.* **108**, 033004 (2012).
- [27] C. H. Greene, *Phys. Rev. A* **42**, 1405 (1990).
- [28] H. Stapelfeldt and H. K. Haugen, *Phys. Rev. Lett.* **69**, 2638 (1992).
- [29] M. Scheer, J. Thøgersen, R. C. Bilodeau, C. A. Brodie, H. K. Haugen, H. H. Andersen, P. Kristensen, and T. Andersen, *Phys. Rev. Lett.* **80**, 684 (1998).
- [30] C. F. Fischer and D. Chen, *J. Mol. Struct.: THEOCHEM* **199**, 61 (1989).
- [31] C. Bahrim, U. Thumm, A. A. Khuskivadze, and I. I. Fabrikant, *Phys. Rev. A* **66**, 052712 (2002).
- [32] W. A. van Wijngaarden and J. Li, *J. Quant. Spectrosc. Radiat. Transfer* **52**, 555 (1994).
- [33] J. E. Sansonetti, *J. Phys. Chem. Ref. Data* **38**, 761 (2009).
- [34] S. Civiš, M. Ferus, P. Kubelík, P. Jelínek, V. E. Chernov, and M. Y. Knyazev, *J. Opt. Soc. Am. B* **29**, 1112 (2012).
- [35] C. Diehl, K. Wendt, A. O. Lindahl, P. Andersson, and D. Hanstorp, *Rev. Sci. Instrum.* **82**, 053302 (2011).
- [36] C.-N. Liu, *Phys. Rev. A* **64**, 052715 (2001).
- [37] S. L. Kaufman, *Opt. Commun.* **17**, 309 (1976).
- [38] U. Fano, *Phys. Rev.* **124**, 1866 (1961).
- [39] B. W. Shore, *Phys. Rev.* **171**, 43 (1968).
- [40] C.-N. Liu and A. F. Starace, *Phys. Rev. A* **60**, 4647 (1999).
- [41] S. Civiš, P. Kubelík, P. Jelínek, V. E. Chernov, and M. Y. Knyazev, *J. Phys. B* **44**, 225006 (2011).